VSP

Advanced Robotics 25 (2011) 1311–1330

ADVANCED ROBOTICS

Full paper

Miniature Pneumatic Curling Rubber Actuator Generating Bidirectional Motion with One Air-Supply Tube

Shuichi Wakimoto [a,*], **Koichi Suzumori** [b] **and Keiko Ogura** [b]

[a] Research Core for Interdisciplinary Sciences, Okayama University, 3-1-1 Tsushima-naka, Kita-ku, Okayama, Okayama 700-8530, Japan

[b] Graduate School of Natural Science and Technology, Okayama University, 3-1-1 Tsushima-naka, Kita-ku, Okayama, Okayama 700-8530, Japan

Received 27 April 2010; accepted 4 June 2010

Abstract

Soft actuators driven by pneumatic pressure are promising actuators for mechanical systems in medical, biological, agriculture, welfare fields and so on, because they can ensure high safety for fragile objects from their low mechanical impedance. In this study, a new rubber pneumatic actuator made from silicone rubber was developed. Composed of one chamber and one air-supply tube, it can generate curling motion in two directions by using positive and negative pneumatic pressure. The rubber actuator, for generating bidirectional motion, was designed to achieve an efficient shape by nonlinear finite element method analysis, and was fabricated by a molding and rubber bonding process using excimer light. The fabricated actuator was able to generate curling motion in two directions successfully. The displacement and force characteristics of the actuator were measured by using a motion capture system and a load cell. As an example application of the actuator, a robotic soft hand with three actuators was constructed and its effectiveness was confirmed by experiments.

Keywords

Soft actuator, pneumatic actuator, bidirectional motion, nonlinear analysis

1. Introduction

Generally, mechanical systems consist of rigid components mainly made from metallic materials and these rigid mechanisms strongly support industrial activities. On the other hand, the need for so-called ‘soft’ mechanisms composed by polymer materials has been increasing. This is because they can be used safely in medical, biological and welfare fields, in which fragile and unstable-shaped objects

* To whom correspondence should be addressed. E-mail: wakimoto@act.sys.okayama-u.ac.jp

DOI:10.1163/016918611X574731

must be handled. Soft actuators are key devices in soft mechanisms because they relate directly to contacting or manipulating such objects physically. Actually, many kinds of soft actuators have been investigated and soft rubber actuators driven by fluid pressure have particular advantages; namely, they are lightweight, have high energy density and are non-electrically driven. Basically, rubber pneumatic actuators work by exploiting their anisotropic elasticity, which produces the intended motion. Methods for creating anisotropic elasticity are divided into two categories: application of reinforced fibers or shape contraction of rubber material. Many rubber actuators with anisotropic elasticity have been developed.

The McKibben actuator is a typical pneumatic rubber-type actuator, developed in the 1950s. This actuator consists of a rubber tube covered with a sleeve composed of knitted fibers. Applying air pressure in the tube makes the rubber tube expand in the radial direction and contract in the axial direction in accordance with the angle of the knitted fibers [1]. Generally, this contracting motion and force in the axial direction are used as the actuator's output. On the other hand, Noritsugu *et al.* developed a rotary-type soft actuator [2]. This actuator consists of a silicone rubber bar, a silicone rubber ball, a fiber and a fiber tube. The rubber bar and ball are covered with the fiber tube, and the fiber reinforces it in the bending direction. As a result of this configuration, when pneumatic pressure is applied to the actuator, the ball works as a joint. Experimentally, a maximum bending angle of 100° was confirmed. In addition, Suzumori *et al.* developed a flexible microactuator (FMA) in the 1980s [3]. This actuator consists of a cylindrical silicone rubber reinforced with fibers, which inhibit expansion of the actuator in the radial direction. The actuator has three chambers inside it. By controlling the balance of pneumatic pressure applied to each chamber, the actuator can create bending motion. When the same pressure is applied to all chambers, the actuator extends in the axial direction.

The actuators mentioned above need reinforced fibers in addition to basic rubber material to achieve anisotropic elasticity, and they have been studied and applied to many robot systems [4–12]. However, because of the complexity of their fabrication, miniaturization of these actuators is difficult.

In contrast, micro-size soft actuators without fibers for generating bending motion have been developed. They create anisotropic elasticity through their shape.

Suzumori *et al.* fabricated a fiber-less FMA by using stereolithography and the actuator can generate the same motion as an FMA [13]. It has spoke-shaped rubber parts in chambers to inhibit deformation in the axial direction instead of fibers. Kang *et al.* also used stereolithography to make a soft micro bellows actuator, which they applied in a micro gripper [14]. Konishi *et al.* developed a micro rubber pneumatic finger [15]. This finger consists of two PDMS sheets with an air chamber between them. Supplying air into the chamber makes it swells up like a balloon and work as a joint, and the finger generates bending motion. Using such fingers, a robotics hand was realized. Watanabe *et al.* also developed a balloon-type actuator for retinal pigment epithelium transplantation. This actuator achieved very large deformation and actual *in vivo* experiments using eyeballs were carried out [16]. Ikeuchi *et al.*

developed a bellows-shaped micro active catheter that bends with water pressure. The very small diameter of this catheter (300 μm) was realized by an original process called membrane micro emboss following excimer laser ablation (MeME-X) [17].

These small non-fiber actuators can generate bending deformation and some of them can attain a large bending angle. However, none of them can generate large bidirectional bending motion with only one pressure-supply tube. Accordingly, in the present study, we developed a rubber pneumatic actuator that generates very large bending motion, so-called 'curling motion', in two directions with one air-supply tube without fiber reinforcement. The ideal curling motion can be thought of as the motion that realizes the maximum value of the bending angle divided by the actuator length.

For this purpose, the actuator is designed in the shape of a bellows. This bellows shape is known to effectively generate telescopic motion, which in turn leads to bending motion [14, 17]. Nonlinear Finite element method (FEM) software was used to derive the most efficient bellows shape that enables the actuator to generate curling motion. According to the FEM analysis results, a curling actuator with a radius of about 1.0 mm was manufactured by the following processes: machining molds, rubber molding and rubber bonding with surface modification by excimer light. The characteristics of the fabricated actuator were measured experimentally. In addition, a soft hand consisting of three of these curling actuators was fabricated. The opening and closing motions of the hand activated by applying negative and positive pressure were experimentally confirmed.

2. Actuator Design Using Nonlinear FEM

2.1. Analysis Conditions

Rubber has a highly nonlinear property. Generally, it is, therefore, difficult to analyze its deformation, especially if it includes large deformation. In the present study, utilizing nonlinear FEM software (Marc, MSC), which handles material nonlinearity and geometrical nonlinearity including large deformations, analyses were carried out to find the most efficient design of a rubber pneumatic actuator for generating bidirectional curling motion.

Room temperature vulcanization (RTV) silicone rubber (KE1603A/B; ShinEtsu Silicones) was used as the actuator material and a material test was conducted according to International Organization for Standardization 37 ('Rubber, vulcanized or thermoplastic — determination of tensile stress–strain properties'). The stress–strain curve of the silicone rubber measured by the test is shown by the dotted line in Fig. 1. It shows that the rubber has nonlinear stress–strain characteristics and a breaking stress of 4.3 MPa.

In the FEM analyses, the Monney–Rivlin model was used for approximating the characteristics of the silicone rubber. This model is a typical function for representing rubber characteristics, which is expressed as the energy function W in the

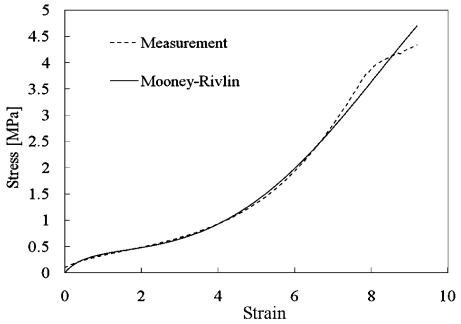

Figure 1. Material property of silicone rubber; dotted line and continuous line are results of the material test and calculations with the Mooney–Rivlin function, respectively.

Table 1.
Coefficients for the Mooney–Rivlin function

Coefficients	Value
C_{10}	0.0863497
C_{01}	0.0621348
C_{11}	−0.0128964
C_{20}	0.00342553
C_{30}	−0.657745

following equations:

$$\begin{aligned} W &= C_{10}(I_1-3)+C_{01}(I_2-3)+C_{11}(I_1-3)(I_2-3) \\ &\quad + C_{20}(I_1-3)^2+C_{30}(I_1-3)^3 \\ I_1 &= \lambda_1^2+\lambda_2^2+\lambda_3^2 \\ I_2 &= \lambda_1^2\lambda_2^2+\lambda_2^2\lambda_3^2+\lambda_1^2\lambda_3^2, \end{aligned} \tag{1}$$

where λ_i represents the compression ratio in each orthogonal direction and C_{ij} represents coefficients depending on material properties.

Table 1 lists the values of C_{ij} derived from the stress–strain curve by a least-squares approach. The continuous line in Fig. 1 represents the energy function W assigned to these coefficients. As the strain approaches breaking point, the test result curve and the Mooney–Rivlin function curve diverge; however, this divergence is not a serious concern because such a large strain area is not used in practice.

To find the most efficient shape of the actuator, the following analysis steps were carried out:

(i) Select fundamental construction of the actuator under positive pressure.

(ii) Determine detailed shape parameters under positive pressure.

(iii) Confirm bidirectional motion generated by positive and negative pressure.

In this paper, pressure unit means gage pressure and no gravity is considered in the analyses.

2.2. Fundamental Design

Efficient actuator design was decided by repeating the cycle of design and analysis. Figure 2 illustrates three actuator models used for determining the fundamental actuator shape. To generate bending motion by a rubber construction without fibers, an asymmetric shape is needed. The cross-sections of all the models are, therefore, a half-moon shape. Basically, the models have a bellows construction on one side (except Model 1, which is the simplest design and has no bellows to confirm the effectiveness of the bellows by comparison). When air pressure is applied to the model, the bellows part can be stretched more easily compared with a flat plate part, which is on the opposite side to the bellows part side. This deformation difference between the two sides generates bending motion of the models. The shape of each model is described in detail as follows:

- Model 1. A half-moon column with a chamber with the same half-moon shape.
- Model 2. A half-moon column with a bellows-shaped chamber.
- Model 3. A bellows-shaped column with a chamber with the same bellows shape.

In all models, the thickness, diameter and length of the rubber are, respectively, 0.15, 2.0 and 15 mm. The top surfaces of the models are fixed. Figure 3 shows the results of nonlinear FEM, where the horizontal axis is air pressure and the vertical axis is displacement (defined as distance of the tip element (shown in Fig. 2a) from its initial position in the x-direction). The maximum displacements of Models 1–3 at a pressure of 50 kPa are 0.04, 0.44 and 9.57 mm, respectively. According to the results for the three models, Model 3 was selected as the fundamental actuator design.

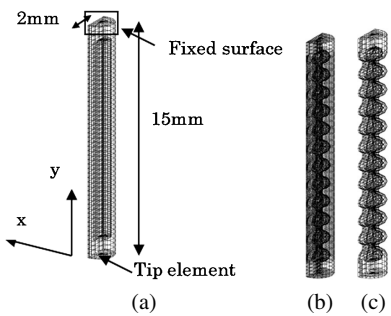

Figure 2. Three analysis models for determining the fundamental shape. (a) Model 1. (b) Model 2. (c) Model 3.

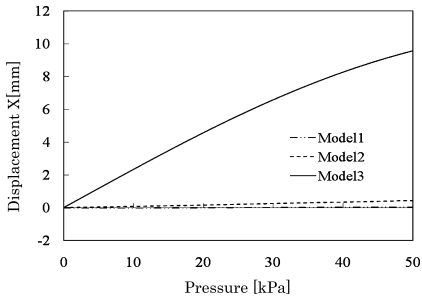

Figure 3. Comparison of three models by nonlinear FEM; the horizontal axis is air pressure and the vertical axis is displacement in the x-direction.

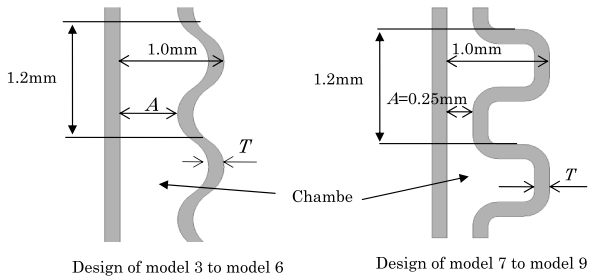

Figure 4. Shape parameters for optimal design.

2.3. Detailed Design

To find an efficient actuator design realizing very large bending motion, six other models (Models 4–9) were analyzed based on Model 3, changing the rubber thickness. In all models, the pitch of the bellows was 1.2 mm and the parameters were defined as shown in Fig. 4. Thickness of the rubber and the minimum chamber radius of the design are represented by T and A, respectively. Table 2 lists T and A for each model.

Models 4–6 were designed with circular lines, because circular lines are easily fabricated with ball-end mills. However, the parameter A cannot be designed arbitrarily, because it depends on the diameter of the end mills. On the other hand, in Models 7–9, the bellows shapes were designed arbitrarily, because of their rectangular lines, which are fabricated with square-end mills. Each A was the same as Model 3.

Figure 5 shows the analysis of the models under various applied air pressures. Figure 5a indicates the displacement of the tip of each model in the x-direction and Fig. 5b is that in the y-direction. In the case of Models 6 and 9, the analysis results stop at around 30 kPa. In addition, the results for Model 5 stop before 50 kPa. With these models, calculation errors appear because the nodes composing one element in the FEM were crossed. These analysis results confirm that in

Table 2.
Shape parameters of bellows

Model	Thickness T (mm)	Minimum chamber radius A (mm)
3	0.25	0.25
4	0.20	0.40
5	0.15	0.55
6	0.10	0.70
7	0.20	0.25
8	0.15	0.25
9	0.10	0.25

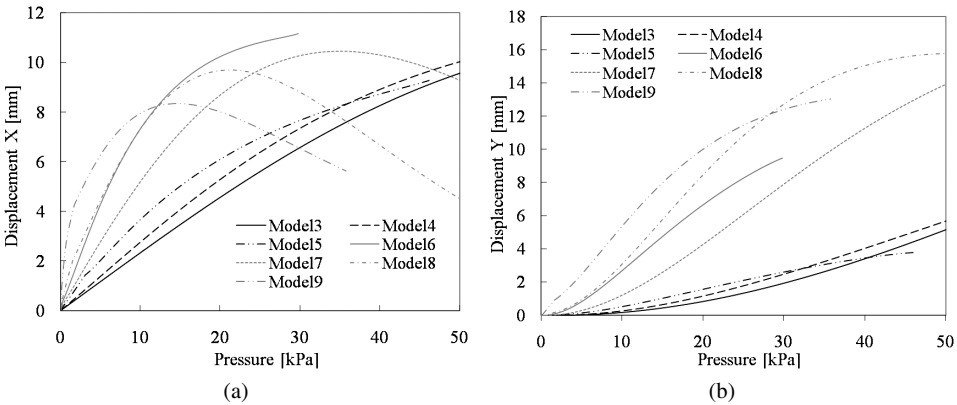

Figure 5. Results of nonlinear FEM of several shape models: (a and b) displacements of the x- and y-directions, respectively.

the case of Models 3–6 the displacements in the y-direction are not enough. Compared with Models 3–6, Models 7–9 generate large displacement in both the x- and y-direction. It seems that their characteristics in the x-direction are inferior to those of Models 4–6 at first glance because the displacement decreases in the second half of the graph in Fig. 5; however, this decreasing trend signifies curling motion (which can be easily understood in Fig. 6d and g). Table 3 shows the bending angle of each model under 30 kPa; Model 8 realizes the largest bending angle θ, which is defined as shown in Fig. 7. In addition, deformations of Model 8 under various positive pneumatic pressures are shown in Fig. 6. Considering actuator applications (e.g., a soft hand), large bending motion is useful to handle objects with unknown size and shape. Therefore, Model 8 was selected as the best actuator design.

2.4. Bidirectional Motion

To confirm the bidirectional motion of Model 8, FEM analysis in the case of applying negative pressure to Model 8 was carried out. Figure 8 shows the results of the

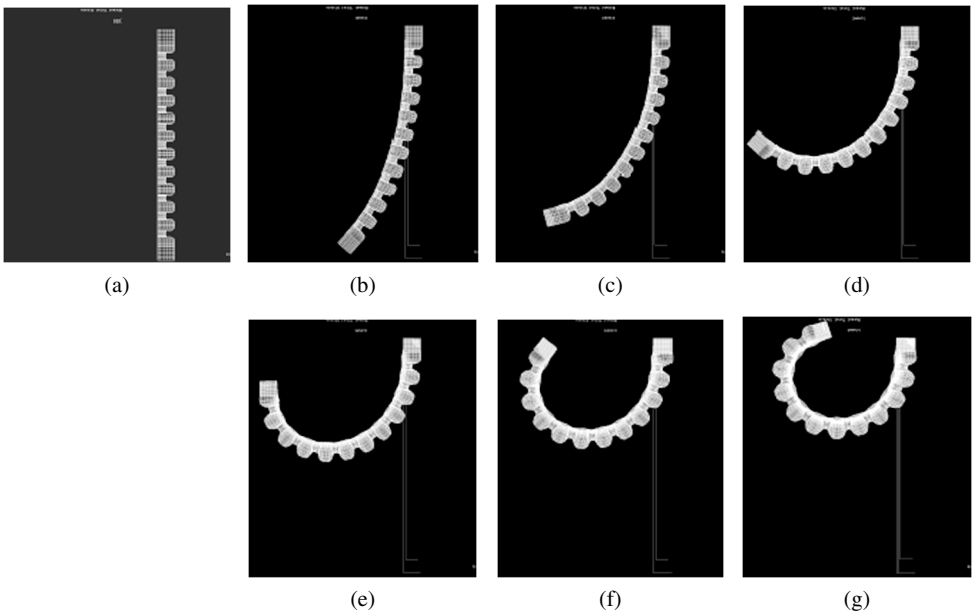

Figure 6. Results of nonlinear FEM with Model 8 under positive pressure. (a) 0 kPa; (b) 5 kPa; (c) 10 kPa; (d) 20 kPa; (e) 30 kPa; (f) 40 kPa; (g) 50 kPa.

Table 3.
Bending angle θ under 30 kPa

Model	θ (rad)
3	0.46
4	0.53
5	0.55
6	1.11
7	0.96
8	1.31
9	1.19

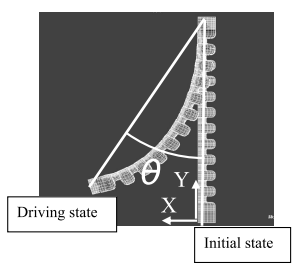

Figure 7. Definition of bending angle θ.

analysis of Model 8 under applied pressure from 0 to −12 kPa. The bellows part can be contracted by negative pressure easily, but the plate side does not deform much. The model, therefore, generates curling motion in the opposite direction to that generated by positive pressure. Under −12 kPa applied pressure, both ends of the model almost make contact.

The trajectory of Model 8 under positive and negative applied pressure is shown in Fig. 9 (see analysis data). The plots are every 5 kPa in positive pressure and −2 kPa in negative pressure. The horizontal axis is the x-direction and the vertical

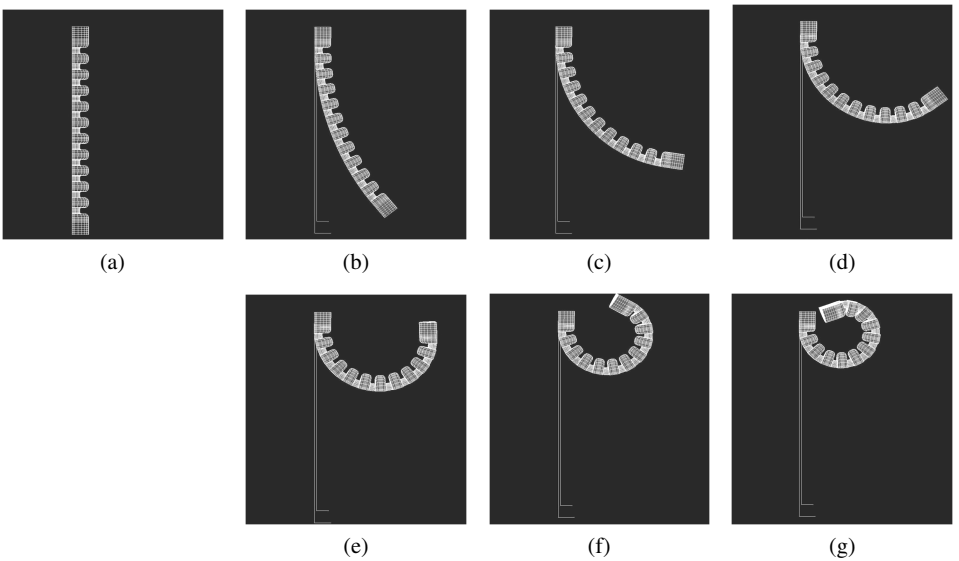

Figure 8. Results of nonlinear FEM with Model 8 under negative pressure. (a) 0 kPa; (b) −2 kPa; (c) −4 kPa; (d) −6 kPa; (e) −8 kPa; (f) −10 kPa; (g) −12 kPa.

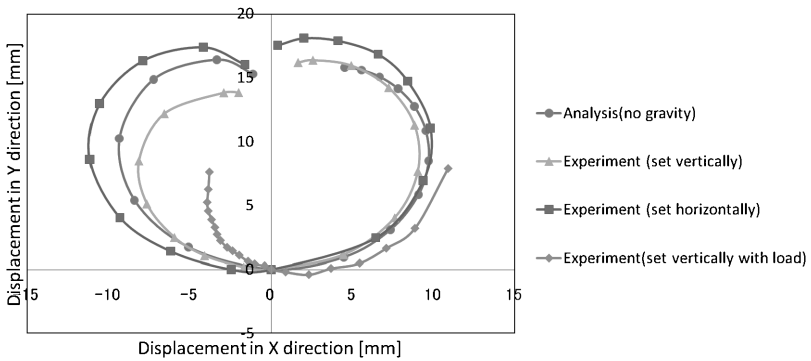

Figure 9. Comparison of experimental results and analytical results on static characteristics of the actuator under positive and negative pressure.

axis is the y-direction. It is clear that the model can generate curling motion in both the clockwise and counter-clockwise direction.

3. Fabrication Process

In consideration of the results of the FEM analysis described above, Model 8 was selected for fabrication. The curling actuator based on Model 8 is configured by two silicone rubber parts: a bellows part (containing chamber space) and a plate part. Figure 10 schematically shows the fabrication process. The bellows part and the plate part are manufactured by molding. The two parts are then bonded by using excimer light.

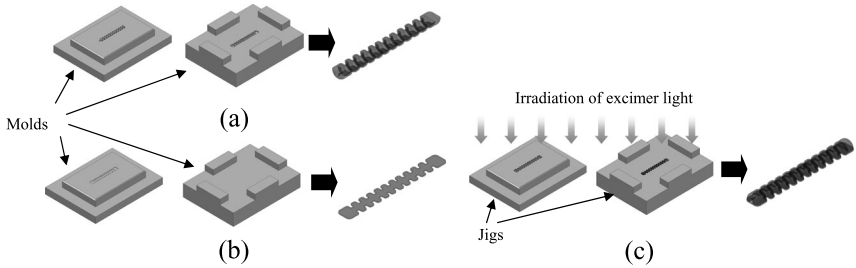

Figure 10. Fabrication process for the curling actuator. (a) Molding of bellows part. (b) Molding of plate part. (c) Bonding of half-bellows and plate parts.

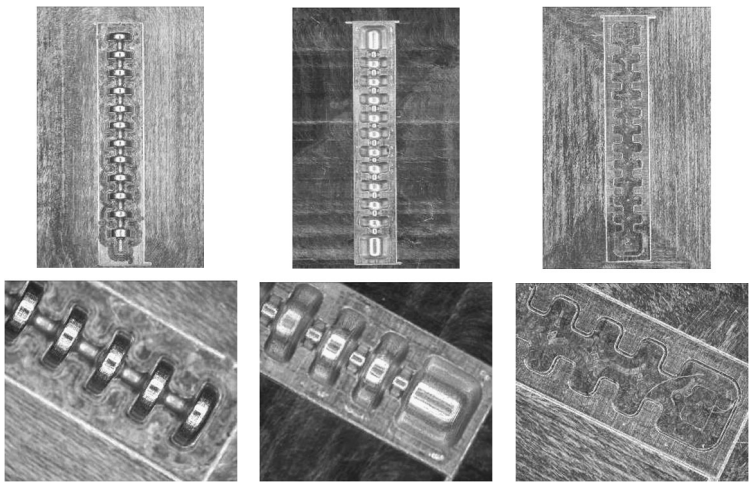

Figure 11. Molds for making the bellows part and plate part.

3.1. Molding Process

The molds were made by micro machining with an accuracy of 10 μm. Compared with the microelectromechanical system process, the molding process is inferior in terms of accuracy; however, it is remarkably easy and automatic, even if the design has a curved shape in the depth direction for the worked surface. The images in Fig. 11a–c, respectively, show the convex mold for the bellows part the concave mold for the bellows part and the concave mold for the plate part. The molds are made of duralumin.

To make the bellows part, RTV silicone rubber in liquid form was poured into the concave mold and air bubbles were removed by vacuuming. After that, the convex mold was combined. Next, the combined molds were set in a furnace. The rubber reached the elastic state by heating at 80°C after 10 min (or at room temperature (23°C) for 24 h). By the same process, the plate part was also manufactured using concave molds and a flat surface mold.

3.2. Rubber Bonding Process

To create the actuator, the two parts (i.e., the bellows part and the plate part) must be bonded. However, it is difficult to bond them with adhesive materials because the adhesive might infill the chamber. Moreover, the material property of the boundary area between the parts changes, so it is possible that the area will burst easily because of its low braking stress property.

In consideration of these problems, the bonding of the rubber parts was realized by chemical surface modification using excimer light (i.e., ultraviolet light with a center wavelength of 172 nm). The light generates ozone, from which radical oxygen is generated. On irradiating the surface of the rubber parts with the excimer light, the photon energy of the ultraviolet and the radical oxygen cut intermolecular links of the rubber, and polar functional hydroxyl groups are formed on the surface. On contact, the surfaces of the two rubber parts become attached chemically by strong hydrogen bonding of these hydroxyl groups [18]. Elasticity in the bonding area is equivalent to that of silicone rubber.

For the above-described bonding process, jigs are needed to achieve precise alignment of the two rubber parts, as shown in Fig. 10c. Concave molds for the bellows part (Fig. 11b) and plate part (Fig. 11c), which have locating parts formed in advance, are used as jigs. The two fabricated rubber parts are reset in the concave molds and the bonding surfaces are turned up. The excimer light is then applied for 3 min. After that, by combining the two molds (containing the rubber parts), the surfaces of the rubber parts are contacted and, 1 h later, the parts are bonded perfectly. On fitting an air-supply tube, the actuator is complete.

4. Characteristics of the Curling Actuator

4.1. Experimental Setup for Motion Characteristics

Figure 12 illustrates the experimental setup for investigating the displacement characteristics of the curling actuator. Positive and negative pneumatic pressure values generated from an air compressor and a vacuum pump are controlled by regulators and switched using a valve, and the pressure can be applied at arbitrary timing by the other valve. The motion of the actuator is recorded by a camera and the images are processed by commercial image processing software.

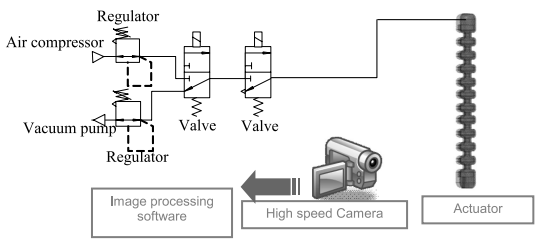

Figure 12. Experimental setup for investigating the curling actuator.

4.2. Static Motion Characteristics

Figure 13 shows the actuator motions, in which gravity is downward. It is clear from Fig. 13 that the actuator can generate very large bending motion in both clockwise and counter-clockwise directions. In addition, Fig. 14 shows the actuator motions in which the actuator is set horizontally (i.e., gravity does not influence in bending direction of the actuator). By comparing Figs 13 and 14, in particular when negative pressure is applied, the curvature of the actuator in Fig. 13 differs at each point, because the stiffness of the actuator becomes lower and the influence of the weight of the actuator increases. However, this phenomenon is not so critical because basically negative pressure is impressed for open motion when the actuator is applied to a hand and also the actuator can adapt its shape to a handled object as shown in Section 5.2.

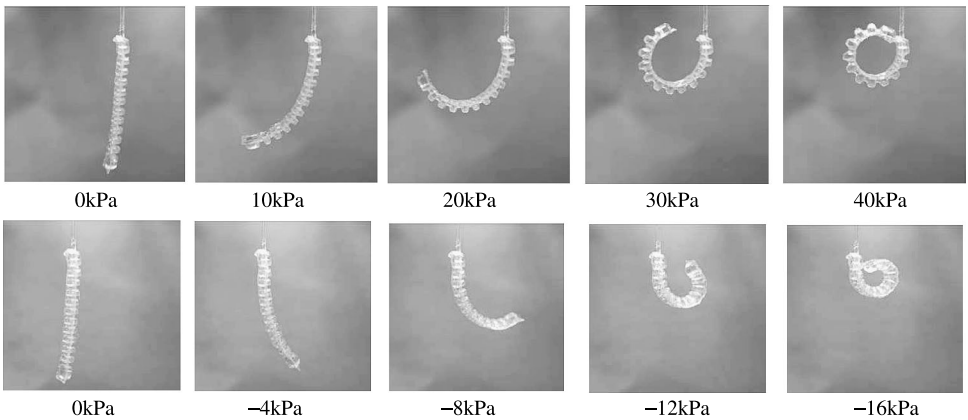

Figure 13. Actuator motions under positive and negative pressure in a vertical setting.

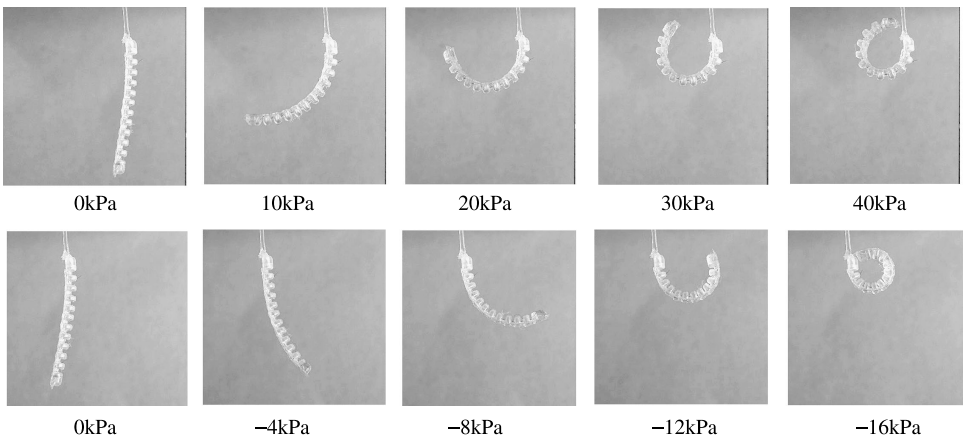

Figure 14. Actuator motions under positive and negative pressure in a horizontal setting.

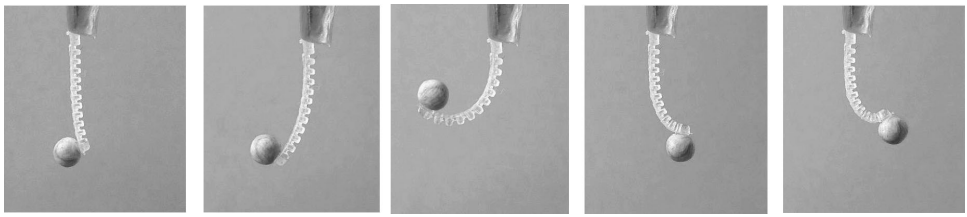

Figure 15. Actuator motions under positive and negative pressure with load.

Figure 15 also shows examples of the actuator motions when a load is added (in Fig. 15 a resin ball of 50 mg in mass and 4 mm in diameter is attached at the actuator tip). As shown in Fig. 15, using the load the displacements become smaller and the curvature differs from in each point strongly.

The analytical and experimental results of the tip trajectory for increasing positive and negative pressure were shown in Fig. 9. The plots are made every 5 kPa under positive pressure and −2 kPa under negative pressure, except for the results with the load in which the plots are made every −4 kPa. The horizontal axis represents the displacement in the x-direction and the vertical axis represents the displacement in the y-direction.

It is very difficult to predict deformation of the rubber by pressure with high accuracy. That is to say, during actual operations like fabrication and driving, all areas of rubber cannot maintain the same shape and state perfectly. Accordingly, if one particular area is deformed slightly earlier than other areas incidentally, that area is deformed significantly before the other areas. Thus, actual accidental phenomena cannot be analyzed. For this reason, the errors between analysis results and experimental results as shown in Fig. 9 occurred. However, trajectory forms of the tips of the analysis model and the fabricated actuator agree well. It can be concluded that, based on the nonlinear FEM, the fabricated rubber actuator can generate bidirectional curling motion with one air-supply tube successfully, even though it is made of silicone rubber only. This is therefore an unprecedented actuator.

Generally, polymer actuators have a relatively large hysteresis. Figure 16a shows the position of the tip of the curling actuator set vertically. The displacements indicated by squares were obtained with increasing positive and negative pressure. The circles represent measured displacement under decreasing positive and negative pressure. Figure 16b and c, respectively, indicate the hysteresis in the x- and y-direction. Considering the applications of the actuator (i.e., it handles fragile and unstable-shaped objects), the hysteresis is small and admissible.

4.3. Dynamic Motion Characteristics

Dynamic characteristics of the actuator were evaluated by using a high-speed camera with a frame rate of 300 frames/s. Figures 17 and 18 indicate the response of the actuator to a step input pressure of 20 and −12 kPa, respectively. A black mark was attached at the tip of the actuator. This mark increased the contrast in the cam-

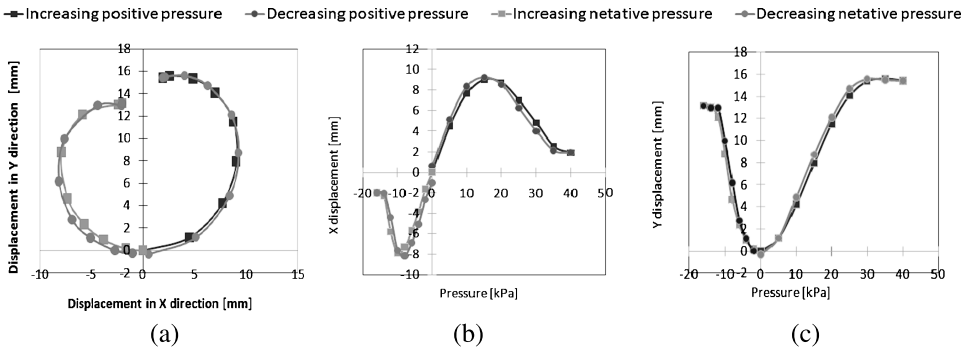

Figure 16. Hysteresis characteristics of curling actuator. (a) Trajectory of tip. (b) Displacement in x-direction. (c) Displacement in y-direction.

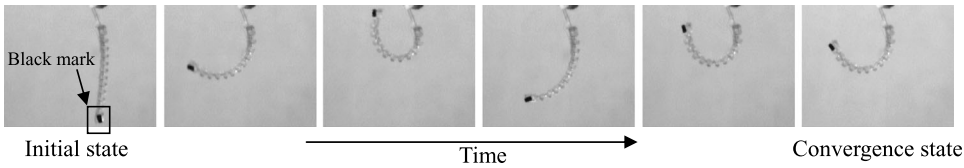

Figure 17. Step response under 20 kPa.

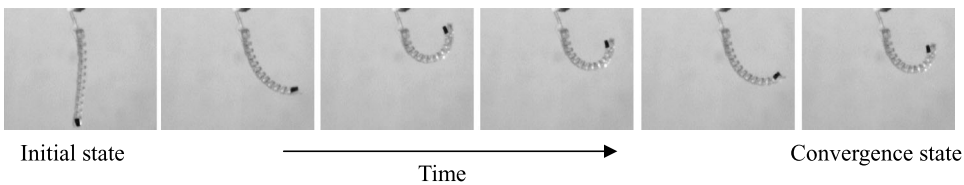

Figure 18. Step response under −12 kPa.

era image. The center point of the mark can be calculated by the image processing software. Displacement of the actuator is defined as the displacement of the center point. In step response experiments, the timepoint of step input was the moment when the voltage was applied to the valve for driving, which is just 1 s after the start of recording. Time (horizontal axis) and absolute displacement of the tip of the actuator from its initial state (vertical axis) are plotted in Fig. 19. A short time delay of within 30 ms and a transient response were observed. The delay is due to the valve response of several milliseconds and the pressure delay from the air-supply tubes. In the measurements of displacement, the two tubes (tubes A and B) were set up as follows. Tube A (inner diameter of 300 μm and length of 20 mm) is connected to the actuator directory; tube B (inner diameter of 500 μm and length of 300 mm) links tube A and the valve. The step response of a bending-type rubber pneumatic actuator has been reported to be oscillatory motion caused by the elastic property and pneumatic characteristics of the actuator [11]. Also, the characteristics of the curling actuator denote oscillatory action. The convergence time until the stable

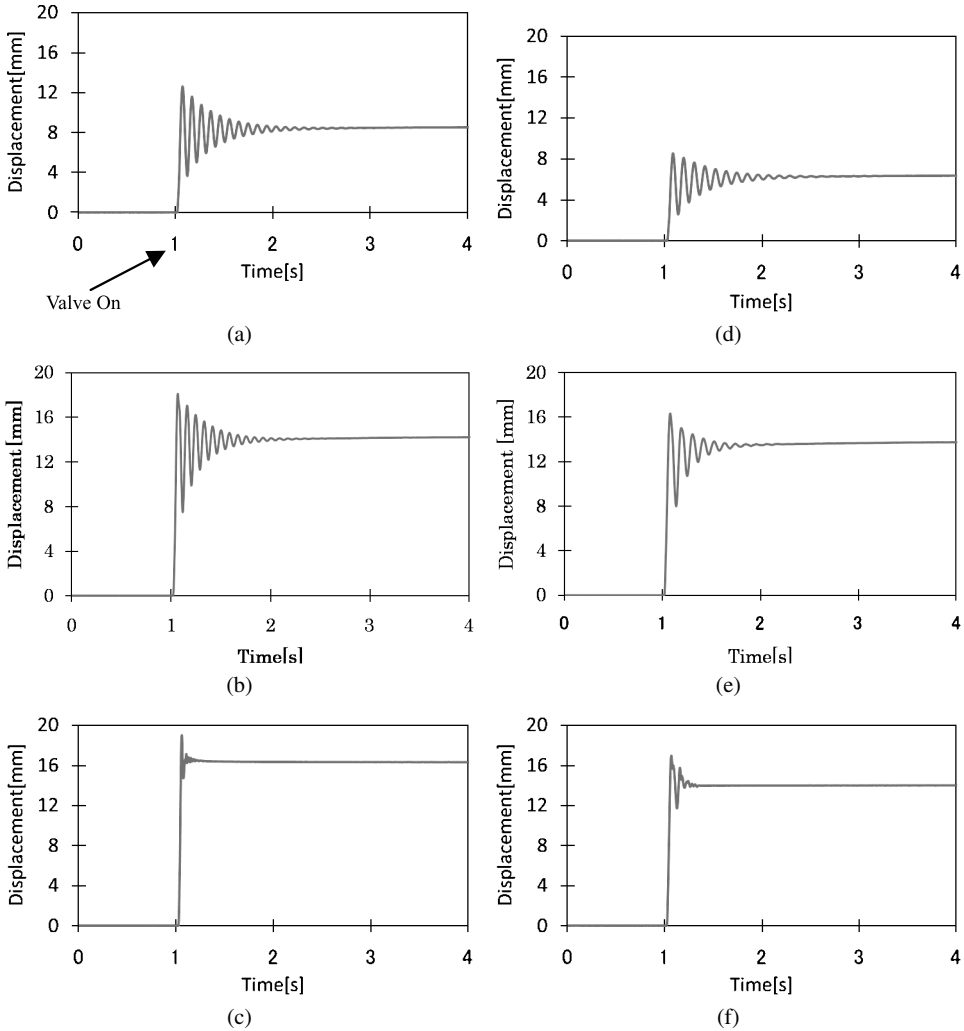

Figure 19. Step response of the actuator. (a) 10 kPa; (b) 20 kPa; (c) 40 kPa; (d) −6 kPa; (e) −12 kPa; (f) −16 kPa.

state is about 1.0 s as shown in Fig. 19a, b, d and e, which represent pressure application of 10, 20, −6 and −12 kPa, respectively. Under applied pressures of 40 and −16 kPa, as shown in Fig. 19c and f, both ends of the actuator contact each other during overshoot and convergence states. For that reason, the convergence time is therefore shorter than other convergence times and the oscillatory characteristics are unstable.

4.4. Force Characteristics

The generated force was measured by a load cell. Although the force that a rubber pneumatic actuator can exert depends not only on pressure, but also on displace-

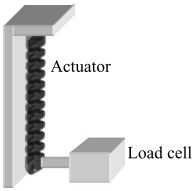

Figure 20. Experimental setup to measure force.

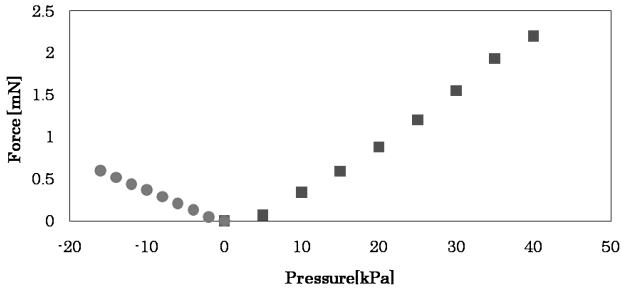

Figure 21. Experimental results of force measurement.

ment or bending angle of the actuators, in this study the maximum force under various pneumatic pressures was measured. To detect the force, the upper end of the actuator was fixed and a plate was set behind the actuator. The load cell was set up to measure the force from the tip of the actuator (Fig. 20). In addition, by replacing the plate with the load cell, the force characteristics under both positive and negative pressure were obtained. Figure 21 plots the measured force of the actuator. The measurement range was from 0 to 40 kPa under positive pressure and from 0 to −16 kPa under negative pressure. The force characteristics are almost linear, and the maximum force is 2.2 mN at 40 kPa and 0.6 mN at −16 kPa.

5. Application as a Soft Hand

5.1. Design and Fabrication

As an application to confirm the effectiveness of the rubber actuator, a soft hand using the actuator was fabricated. The hand has three curling actuators as fingers, whose lengths were set according to the ratio of human fingers; namely, the first (thumb), second (index) and third (middle) fingers are 7.6, 11.2 and 12.4 mm long, respectively. The finger length can be controlled by the number of bellows. The absolute value of the output of displacement depends on the number; however, the essential characteristics of the actuators were not changed, because they depend on the bellows shape. Table 4 lists the number of bellows and the length of each finger. In addition, the second and third fingers are arranged in parallel, but the first finger is set at an angle of 30° to the other fingers in the same manner as a human hand.

To fabricate the hand, four molds are needed. Two of them are shown in Fig. 22. Figure 22a shows the concave mold for the bellows part composed of three fingers, and Fig. 22b shows the concave mold for the plate part, also composed three fingers and two base parts for making a palm, which is a triangular shape. Therefore, the hand can be fabricated by the same steps as for fabricating one actuator as shown in Fig. 10 (it is not needed to fabricate each finger, respectively).

Table 4.
Number of bellows and length of each finger

	Number of bellows	Finger length (mm)
First finger (thumb)	4	7.6
Second finger (index)	7	11.2
Third finger (middle)	8	12.4

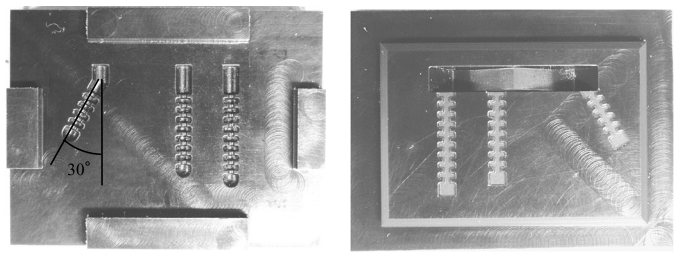

Figure 22. Molds for a robot hand with three fingers. (a) Concave mold for bellows part. (b) Concave mold for plate part.

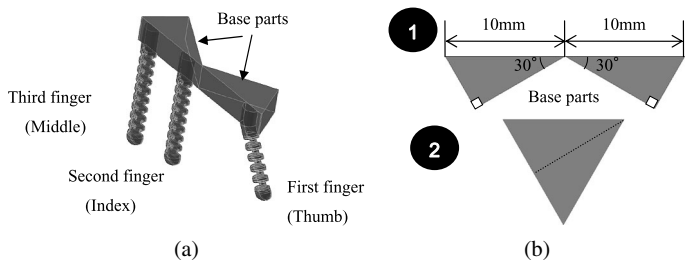

Figure 23. Configuration of a soft hand with three fingers. (a) Hand state before folding. (b) Folding concept.

After the rubber parts are molded and bonded, the hand is formed as shown in Fig. 23a. Then, by folding the two base parts as shown in Fig. 23b, the hand can be realized.

5.2. Demonstration

Using the developed soft hand, handling demonstrations were carried out. As the actuator can generate bidirectional motion, the hand can perform opening and closing motions as shown in Fig. 24a. Moreover, since the hand has low mechanical impedance, it can pick up a fish egg (diameter 5 mm; mass 0.15 g) successfully without breaking it, as shown in Fig. 24b. In addition, performing opening motion, the hand can hold a large object (mass 0.15 g) as shown in Fig. 24c.

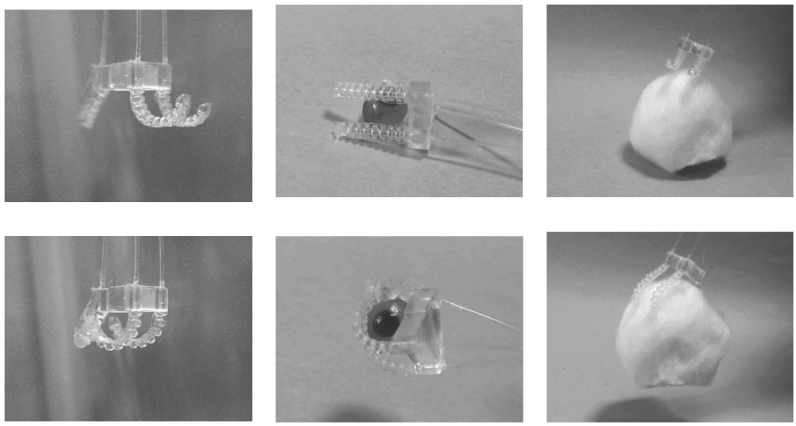

(a) (b) (c)

Figure 24. Experiments with a soft hand. (a) Open and close motion. (b) Grasping fish egg. (c) Holding up large object.

6. Conclusions

A novel pneumatic rubber actuator that can generate bidirectional curling motion by one air-supply tube was developed.

The appropriate design for generating the motion was derived by nonlinear FEM analysis. In the analysis, the Mooney–Rivlin function was adopted and, as a result, the appropriate actuator design has a bellows shape, which enables very large bending motion in two directions. Based on the analysis results, an actuator was manufactured. The actuator consists of two parts — a bellows part and a plate part — and each part was made by molding. After molding, the two parts were bonded by surface modification using excimer light. By these processes, an actuator with a diameter of 2 mm and length of 15 mm was successfully fabricated with the same design as that determined by nonlinear FEM.

The fabricated actuator generated bidirectional curling motion by means of positive and negative pneumatic pressure. With regard to the static characteristics of the actuator, although some errors appeared, the experimental results agreed with the FEM results well. In addition, the dynamic characteristics of the actuator were measured by a high-speed camera. The step response of the actuator was oscillatory, which is a typical response of rubber pneumatic actuators. Convergence time until the stable state is about 1 s. The force characteristics of the actuator were measured under the condition of no displacement. Maximum force under positive pressure was 2.2 mN and that under negative pressure was 0.6 mN. Moreover, three of the actuators were applied as a soft robot hand. The softness of the hand allowed it to grasp a tiny fish egg without breaking it. In addition, by performing opening and closing motions generated by negative and positive pressure, it could hold a large object successfully.

Acknowledgements

This research was partially supported by the MEXT program 'Promotion of Environmental Improvement for Independence of Young Researches' under the Special Coordination Funds for promoting Science and Technology and 'Grant-in-Aid for Scientific Research (A) (19206027)'.

References

1. H. F. Schulte, Jr., The characteristics of the McKibben artificial muscle, in: *The Application of External Power in Prosthetics and Orthotics*, pp. 94–115. National Academy of Sciences — National Research Council, Washington, DC (1961).
2. T. Noritsugu, D. Sasaki and M. Takaiwa, Application of artificial pneumatic rubber muscles to a human friendly robot, in: *Proc. IEEE Int. Conf. on Robotics and Automation*, Taipei, pp. 2188–2193 (2003).
3. K. Suzumori, Flexible microactuator (1st report, static characteristics of 3 DOF actuator), *Trans. JSME C* **55**, 2547–2552 (1989) (in Japanese).
4. C. P. Chou and B. Hannaford, Measurement and modeling of McKibben pneumatic artificial muscles, *Trans. Robotics Automat.* **12**, 90–102 (1996).
5. P. van der Smagt, F. Groen and K. Schulten, Analysis and control of a rubbertuator arm, *Biol. Cybernet.* **75**, 433–440 (1996).
6. K. Kawashima, T. Sasaki, T. Miyata, N. Nakamura, M. Sekiguchi and T. Kagawa, Development of Robot using pneumatic artificial rubber muscles to operate construction machinery, *J. Robotics Mechatron.* **16**, 8–16 (2004).
7. B. Vanderborght, B. Verrelst, R. Van Ham, M. Van Damme, P. Beyl and D. Lefeber, Torque and compliance control of the pneumatic artificial muscles in the biped 'Lucy', in: *Proc. IEEE Int. Conf. on Robotics and Automation*, Orlando, FL, pp. 842–847 (2006).
8. K. Hosoda, T. Takuma, A. Nakamoto and S. Hayashi, Biped robot design powered by antagonistic pneumatic actuators for multi-modal locomotion, *Robotics Autonomous Syst.* **56**, 46–53 (2008).
9. S. Wakimoto, K. Suzumori and T. Kanda, A bio-mimetic amphibious soft cord robot, *Trans. JSME* **71**, 471–476 (2005) (in Japanese).
10. D. Sasaki, T. Noritsugu and M. Takaiwa, Development of active support splint driven by pneumatic soft actuator (ASSIST), *J. Robotics Mechatron.* **16**, 497–503 (2004).
11. K. Suzumori, S. IIkura and H. Tanaka, Flexible microactuator for miniature robots, in: *Proc. IEEE Micro Electro Mechanical Systems*, Nara, pp. 204–209 (1991).
12. K. Suzumori, S. Endo, T. Kanda, N. Kato and H. Suzuki, A bending pneumatic rubber actuator realizing soft-bodied manta swimming robot, in: *Proc. IEEE Int. Conf. on Robotics and Automation*, Rome, pp. 4975–4980 (2007).
13. K. Suzumori, A. Koga and R. Haneda, Microfabrication of integrated FMAs using stereo lithography, in: *Proc. Micro Electro Mechanical Systems*, Oiso, pp. 136–141 (1994).
14. H. W. Kang, I. H. Lee and D. W. Cho, Development of a micro-bellows actuator using microstereolithography technology, *Microelectron. Eng.* **83**, 1201–1204 (2006).
15. S. Konishi, M. Nokata, O. C. Jeong, S. Kusuda, T. Sakakibara, M. Kuwayama and H. Tsutsumi, Pneumatic micro hand and miniaturized parallel link robot for micro manipulation robot system, in: *Proc. IEEE Int. Conf. on Robotics and Automation*, Orlando, FL, pp. 1036–1041 (2006).

16. Y. Watanabe, M. Maeda, N. Yaji, R. Nakamura, H. Iseki, M. Yamamoto, T. Okano, S. Hori and S. Konishi, Small, soft, and safe microactuator for retinal pigment transplantation, in: *Proc. IEEE Micro Electro Mechanical Systems*, Kobe, pp. 659–662 (2007).
17. M. Ikeuchi and K. Ikuta, Development of pressure-driven micro active catheter using membrane micro emboss following excimer laser ablation (MeME-X) process, in: *Proc. IEEE Int. Conf. on Robotics and Automation*, Kobe, pp. 4469–4472 (2009).
18. K. Kikuchi and N. Hishinuma, Ozone process and UV process, in: *Surface Treatment Technology Hand Book*, H. Mizumati, M. Tobayama, K. Naito, T. Tanaka, T. Matsunaga and E. Yanagihara (Eds), pp. 526–538. NTS, Tokyo (2001) (in Japanese).

About the Authors

Shuichi Wakimoto received the BE, ME and DE degrees from Okayama University, Japan, in 2002, 2004 and 2007, respectively. From 2004 to 2007, he was a Research Fellow of the Japan Society for the Promotion of Science. From 2007 to 2009, he was an Assistant Professor at the Graduate School of Natural Science and Technology, Okayama University. From 2009 to 2011, he was an Assistant Professor and since 2011 he has been an Associate Professor at the Research Core for Interdisciplinary Sciences, Okayama University, Japan. His research interests are flexible actuators and their applications. He is a Member of the Japan Society of Mechanical Engineers and the Robotics Society of Japan.

Koichi Suzumori received the BS, MS and PhD degrees in Mechanical Engineering from Yokohama National University, Japan, in 1982, 1984 and 1990, respectively. He worked for Toshiba R&D Center from 1984 to 2001, and also worked for the Micromachine Center, Tokyo, from 1999 to 2001. He has been a Professor of the Graduate School of Natural Science and Technology, Okayama University, Japan, since 2001. He is mainly engaged in the research fields of new actuators and their applications. He has received many awards, such as the JSME Medal for Outstanding Paper, in 1999, RSJ Best Paper Award, in 2000, and JSAEM Best Book Award, in 2006. He is a Fellow Member of the Japan Society of Mechanical Engineers.

Keiko Ogura received the BE and ME degrees from Okayama University, Japan, in 2007 and 2009, respectively. Since 2009, she has worked for OMRON in Japan.